CHEMICAL ENGINEERING TRANSACTIONS
VOL. 70, 2018
A publication of AIDIC
The Italian Association of Chemical Engineering
Online at www.aidic.it/cet
Guest Editors: Timothy G. Walmsley, Petar S. Varbanov, Rongxin Su, Jiří J. Klemeš

ISBN 978-88-95608-67-9; **ISSN** 2283-9216
DOI: 10.3303/CET1870138

Energy Saving Potential and the Efficacy of Using Different Control Strategies for the Heat Exchanger Network Operation

Marian Trafczynski*, Mariusz Markowski, Krzysztof Urbaniec, Robert Grabarczyk

Institute of Mechanical Engineering, Faculty of Civil Engineering, Mechanics and Petrochemistry, Warsaw University of Technology, Lukasiewicza 17, 09-400 Plock, Poland
Marian.Trafczynski@pw.edu.pl

Heat exchangers – typically arranged in heat recovery networks – belong to the devices most widely used in industrial production systems. The control performance of heat exchanger network (HEN) operation can be impaired by fouling which builds up on heat-exchange surface. Fouling leads to burning extra fuel to compensate for reduced heat recovery and induces increased costs of cleaning interventions, etc. In this work, a real-life benchmark system is considered. The controlled system represents a HEN coupled with a crude distillation unit (CDU). The mathematical model of HEN with stream splits and interactions between the branches, was built and validated based on real-life data recorded during CDU operation. The use of various control strategies (employing linear control systems with PID controllers) for HEN operation was studied with the aim to maximize heat recovery in the HEN involving splits. Using historical data on HEN operation, simulations of closed-loop control were performed in MATLAB/Simulink environment. The simulation results demonstrated the efficacy of the studied strategies and their potential to achieve energy savings in CDU operation.

1. Introduction

In industrial production systems, the control performance of heat exchanger network (HEN) operation can be impaired by fouling which builds up on heat-exchange surfaces. Fouling leads to burning extra fuel to compensate for reduced heat recovery and induces increased costs due to cleaning interventions (Markowski and Urbaniec, 2005), etc. According to literature sources, various approaches to the mitigation of fouling effects in industrial heat exchangers (HEs) and HENs (Smith et al., 2017) stem from the fact that apart from fouling-induced reduction of steady-state heat recovery, transient states of HEs and inefficient control of both individual HEs and entire HENs may also have a detrimental effect on the overall performance of the HEN. Energy savings and operational optimization attracted high interest of researchers in the past two decades (Klemeš and Varbanov, 2013). Model predictive control (MPC) represents state-of-art in model-based control. As the HEs have various uncertain parameters, robust MPC can optimize the control performance subject to uncertainties. Linear matrix inequalities (LMIs) serve to formulate a convex optimization problem in the form of semidefinite programming (SDP) that is solved efficiently in polynomial time. Vasičkaninová et al. (2011) designed the neural network predictive control (NNPC) structure for the HEs to ensure energy savings. Bakošová and Oravec (2014) designed LMI-based robust MPC for the HEN. Simulation of the closed-loop control performance confirmed the possibility to assure energy savings. Oravec et al. (2017) presented the robust MPC with integral action implemented to the control of the HEs in the presence of fouling. The simulation results confirmed significant improvement of the control performance and a reduction in the oscillation behaviour, compared to the original PID control strategy.
In this work, an industrial benchmark system is considered. The controlled system represents HE units from a network coupled with a CDU (see Figure 1). The mathematical model was built and validated based on the data recorded during CDU operation. Aiming at the maximization of heat recovery in the HEN, one has to account for the detrimental effect of deposits mounting up on the heat transfer surfaces of the HEs and for the influence of process parameters (temperature, mass flow, etc.) that may change with time. To this end, the present authors propose using simple decentralised control configurations (control loops with PID Controllers). In order to save energy, the control objective is to maximize heat recovery, understood as total heat flow Q transferred

Please cite this article as: Trafczynski M., Markowski M., Urbaniec K., Grabarczyk R., 2018, Energy saving potential and the efficacy of using different control strategies for the heat exchanger network operation , Chemical Engineering Transactions, 70, 823-828
DOI:10.3303/CET1870138

in the HEN; this can be done by keeping end temperatures T_{ABend} and T_{CDend} after parallel branches AB and CD, respectively, as high as possible (see Figure 1).
The following simple control strategies (known to be of interest to plant Operators) were investigated:

- Keeping the values of split ratio in branch pairs AB and CD constant.
- For both AB and CD, keeping constant temperature at the outlet from one of the two parallel branches.
- For both AB and CD, keeping outlet temperatures of the parallel branches equal.
- So-called self-optimizing control based on the idea presented by Jäschke and Skogestad (2014).

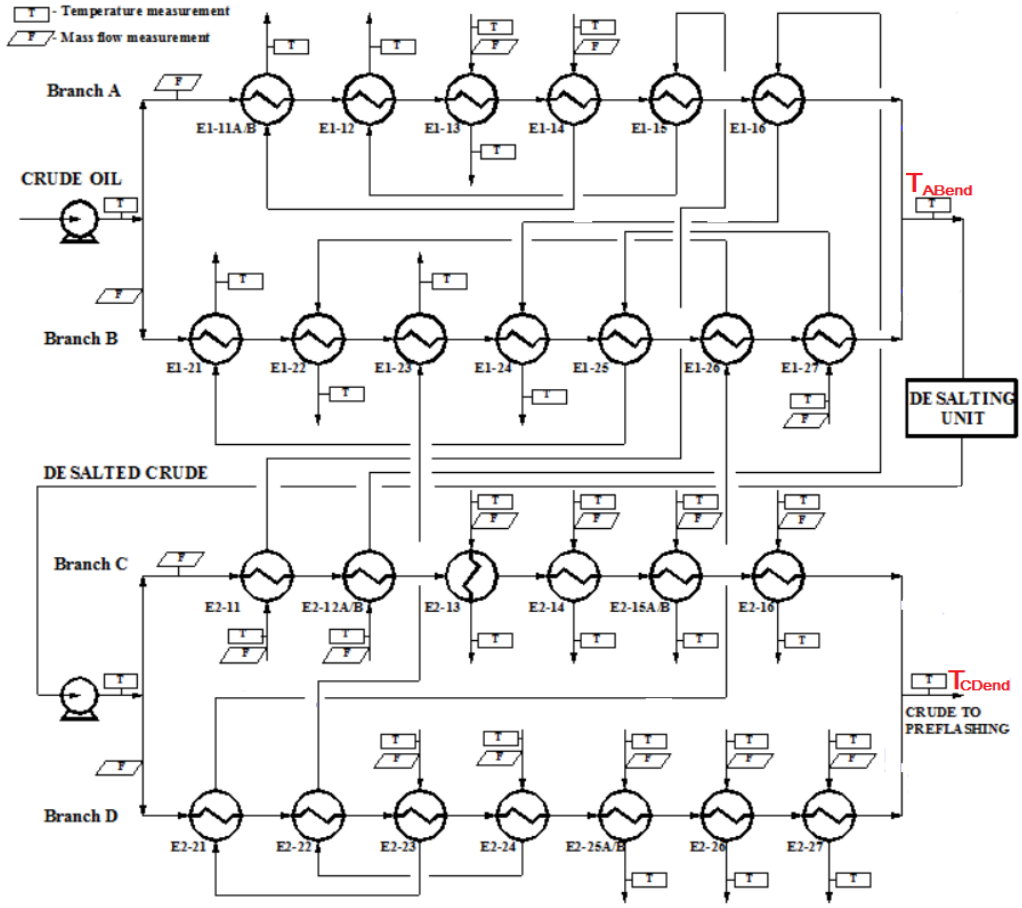

Figure 1: Scheme of the HEN with the parallel branches AB and CD

2. Dynamic model of a shell-and-tube HEN

The planning of efficient use of HEs under changing operating conditions (e.g., conditions resulting from fouling build-up with time) requires the application of adequate dynamic models. The research described below was based on the mathematical model proposed by Trafczynski et al. (2016), of transient heat exchange with the influence of thermal resistance of fouling taken into account. The dynamic HEN model was developed and used as a tool for simulation of HEN operation with studied simple control strategies (Figure 2).

2.1 Model equations

A shell-and-tube HE was considered as an array of cells in which the exchange of heat was modelled using the lumped-parameter approach (Varbanov et al., 2011). Model equations to describe transient states of the HE were derived from the energy balance of a control volume in which changes in the state of tube-side fluid, tube walls and shell-side fluid were accounted for. The energy balance of the entire cell numbered (*j,k*) (*j-th* heat exchanger pass, *k-th* channel between baffles) was represented by three ordinary differential equations (Varga et al., 1995). In order to take the influence of fouling on the heat transfer into account, heat transfer coefficients were calculated using the formulae that include thermal resistances of the tube-side and shell-side fouling layers. As the equations were solved, transfer functions were obtained to describe the relationships between input signals (changes in process parameters at HE inlet) and responses (changes in temperature at HE outlet).

Upon linearization of the equations, Laplace transforms were obtained for each HE cell. This approach has the advantage of yielding simple analytical relationships which are sufficiently accurate as long as the number of cells defined in the HE structure is large. The model was validated using operational data of a real-life HEN coupled with a CDU. The values of simulated and real temperature at HE outlet in transient states of the HE were compared and found to be in close agreement. For more details of the dynamic model of a shell-and-tube HE, please refer to the work (Trafczynski et al., 2016).

2.2 Implementation of the dynamic HEN model in Matlab-Simulink

By solving the equations of the mathematical model, relationships employing operator transmittances can be obtained between disturbances occurring at cell inlet and changes in temperature at cell outlet. Operator transmittance *G(s),* where *s* denotes complex variable, is a widely used tool for describing a dynamic system. It is defined as a ratio of the output signal Laplace transform *y(s)* to the input signal Laplace transform *u(s)*, assuming that the initial conditions are equal to zero: $G(s)=y(s)/u(s)$. Each cell is subjected to four input signals (tube-side and shell-side inlet temperatures $T_{ti(j,k)}$, $T_{si(j,k)}$ and mass flows M_t, M_s) and generates two output signals (tube-side and shell-side outlet temperatures $T_{to(j,k)}$, $T_{so(j,k)}$). Therefore, in the model of a HE, each cell is represented by eight operator transmittances (ratios of the output signal to the input signal): $G_1(s)=T_{so}/M_t$, $G_2(s)=T_{so}/M_s$, $G_3(s)=T_{so}/T_{si}$, $G_4(s)=T_{so}/T_{ti}$, $G_5(s)=T_{to}/M_t$, $G_6(s)=T_{to}/M_s$, $G_7(s)=T_{to}/T_{si}$, $G_8(s)=T_{to}/T_{ti}$. As three ordinary differential equations presented by Varga et al. (1995) include products of the controlled variable and input variables, these relationships are non-linear but can be linearized by Taylor series expansion in the neighborhood of the average values of variables. After subsequent Laplace transformation in the time domain, differential equations are transformed into algebraic ones making it possible to obtain operator transmittances for cell *(j,k)* – see reference (Trafczynski et al., 2016). Prior to developing the computer-aided dynamic model, a detailed block diagram of the HEs and the entire HEN should be developed to visualize the interdependences between exchanger cells and between HEs in the HEN. As each HE in the HEN is considered as a set of several cells connected in accordance with the chosen flow arrangement, the complete block scheme is rather complex. The developed block diagram of the HEN based on the operator transmittances could be implemented and converted into a simulation tool using Simulink software in MATLAB environment. A prerequisite for that was the availability of a database containing steady-state values of the operation parameters in all the cells (Trafczynski et al., 2016), of all the HEs in the HEN.

3. Energy saving potential analysis

In order to investigate the energy saving potential of a proposed control strategies for HEN operation, four branches ABCD (the crude preheat trains) were selected from a real-life HEN coupled with a CDU rated 110 kg/s of crude oil. Twenty-six shell-and-tube, two-pass HEs with straight tubes and floating heads are connected as schematically shown in Figure 1. Using operational data available from a selected time interval of continuous HEN operation, HE characteristics were studied at the stage of fouling build-up after one year (passed from operation start-up when HE surfaces had been clean). Owing to limited measurement data, it was not possible to determine the relationship between the thermal resistance of fouling R_f (fouling factor) and time *t,* for each HE. (The measurements of temperature and mass flow were performed only at the inlet and outlet of the studied HEN but no temperature measurements were available between the HEs – see Figure 1.) In order to resolve this issue, the R_f values of HEs that were used in the simulation studies had been postulated by the authors on the basis of values recommended by TEMA standards (Table 1).

As shown in the HEN scheme in Figure 1, the crude oil feed stream is split in parallel branches A and B before the desalting unit, and in parallel branches C and D after the desalting unit. These branches are composed of HEs in which heat from the distillation products is recovered. In the studied CDU unit, energy-optimal operation of the HEN could not be reached because the split ratios in the parallel branches were arbitrarily kept constant to ensure near 50% (periodically changed by the plant Operator) of the total mass flow of crude oil in each branch. This control strategy, preferred by the plant Operator, was named – control strategy no. 0. The following control strategies were investigated and compared to the control strategy no. 0:

- Keeping the values of split ratio in branch pairs AB and CD constant and equal 50 % of the total mass flow of crude oil in each branch – control strategy no. 1 (Figure 2a).
- For both AB and CD, keeping constant temperature at the outlet from one of the two parallel branches – control strategy no. 2 (Figure 2b).
- For both AB and CD, keeping outlet temperatures of the parallel branches equal – control strategy no. 3 (Figure 2c).
- So-called self-optimizing control based on the idea presented by Jäschke and Skogestad (2014) – control strategy no. 4 (Figure 2d).

Table 1: Values of the fouling resistance and heat transfer coefficient for the studied HEs

HE No.	Fouling factor R_f×10^{-3} (m^2K/W) after period of 1 year of operation	Total heat transfer coefficient for clean HE *U* (W/m2K)	HE No.	Fouling factor R_f×10^{-3} (m^2K/W) after period of 1 year of operation	Total heat transfer coefficient for clean HE *U* (W/m2K)
E1-11A	0.926	693	E2-12A	0.801	691
E1-11B	0.890	762	E2-12B	0.625	706
E1-12	0.681	572	E2-13	1.332	56
E1-13	1.011	363	E2-14	0.913	346
E1-14	0.846	831	E2-15A	0.679	426
E1-15	0.869	633	E2-15B	0.894	446
E1-16	0.834	636	E2-16	0.900	518
E1-21	1.104	546	E2-21	0.678	858
E1-22	0.700	810	E2-22	0.828	467
E1-23	0.753	417	E2-23	0.592	891
E1-24	0.679	648	E2-24	0.926	502
E1-25	0.951	649	E2-25A	0.900	653
E1-26	0.992	898	E2-25B	0.782	692
E1-27	0.913	678	E2-26	0.931	280
E2-11	0.608	691	E2-27	0.900	197

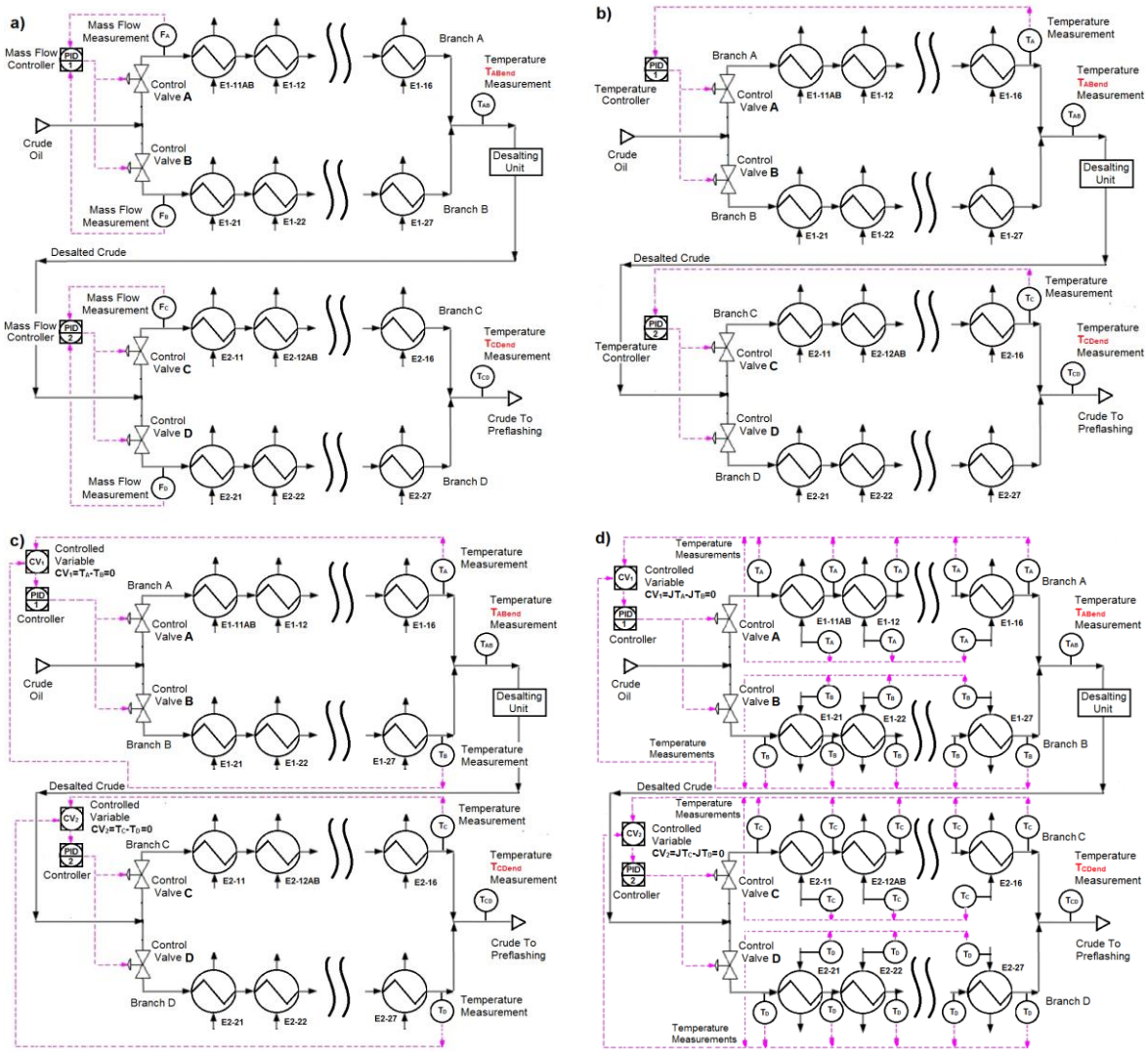

Figure 2: Schemes of the HEN with PID-control loops implemented in Simulink/MATLAB, a) refers to the control strategy no. 0 and 1, and b), c), d) refer to the control strategies no. 2, 3, and 4, respectively

For all proposed control strategies (see Figure 2), for PID-control loops 1 and 2 the manipulated variables are split ratios in branch pairs AB and CD. For the control strategy no. 2, the controlled variables are temperatures at the outlet from one of the two parallel branches; T_A and T_C for PID-control loops 1 and 2, respectively (see Figure 2b). For the control strategy no. 3, the controlled variables are CV_1 and CV_2. These variables are defined as the differences between the studied outlet temperatures: $CV_1=T_A-T_B$ and $CV_2=T_C-T_D$ for PID-control loops 1 and 2, respectively (see Figure 2c). For the control strategy no. 4, the controlled variables are defined as the differences between the *Jäschke Temperatures, JT* (for more details please refer to Jäschke and Skogestad, 2014): $CV_1=JT_A-JT_B$ and $CV_2=JT_C-JT_D$ for PID-control loops 1 and 2, respectively (see Figure 2d).
PID controllers 1 and 2 were separately tuned according to the SIMC tuning rules (Skogestad, 2003), by assuming step (10 %) increases in the crude oil mass flows (+6.11 kg/s in M_{At} and M_{Ct}) in each of the branches A and C. The open-loop step responses of the controlled variables were obtained and the resulting values of the tuning parameters for PID controllers are presented in Table 2.
Using real operational data from the selected period of five days of continuous HEN operation, the simulations of closed-loop control were performed and the results enabled comparative evaluation of the studied strategies and their potential to achieve energy savings in CDU operation – see Figures 3 and 4.

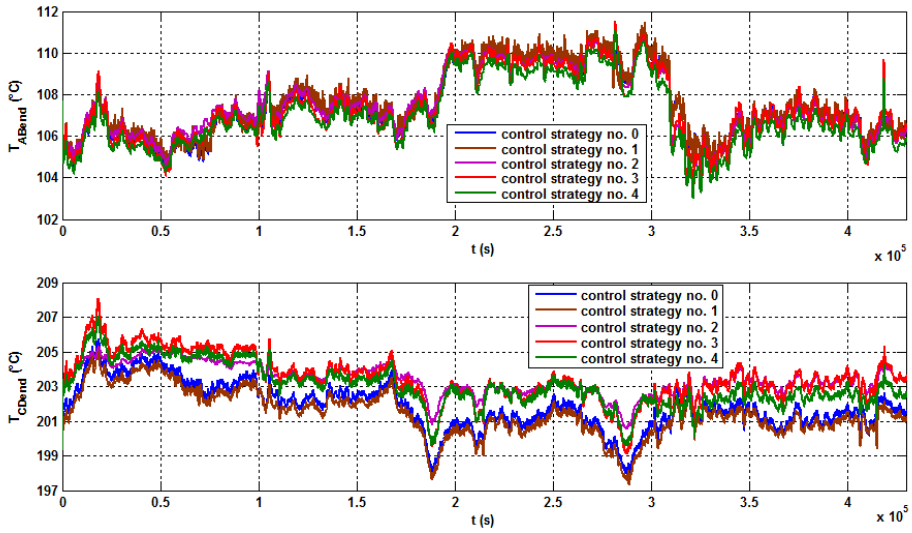

Figure 3: Outlet temperatures from the parallel branches versus operational time

Figure 4: Outlet temperature increments versus operational time

As shown in Figure 3, the application of the proposed control strategies no. 2, 3 and 4 resulted in an increase in the outlet temperature only from CD branches (T_{CDend}), while the outlet temperature from AB branches (T_{ABend}) oscillates around the temperature values recorded for the control strategy no. 0. This situation results from the fact that the same hot streams first pass through the HEs in the CD branches and then through the HEs in the AB branches – please refer to Figure.1. Thus, as a result of the proposed control strategies, the heat exchange increases in HEs of branches CD, so the hot streams deliver more heat and become cooler, and then the cooler hot streams go to the HEs of branches AB, causing no significant increase in the outlet temperature T_{ABend}. Moreover, the application of strategy of keeping the values of split ratio in branch pairs AB and CD constant and

equal 50 % of the total mass flow of crude oil in each branch (control strategy no. 1) resulted in an decrease in the outlet temperatures from AB and CD branches.
As shown in Figure 4, in the studied period of CDU operation, the crude oil outlet temperature increment dT_{CDend} fluctuated in range 0-3 °C. The Table 2 contains the results of total heat recovery of HEN, the heat-recovery increments *dQ,* the crude oil outlet temperature increments dT_{CDend} and the average daily energy savings, showing the efficacy of the studied control strategies.

Table 2: The results of the efficacy of the studied control strategies and the PID controller parameters

No. of used control strategy	Total heat recovery of HEN *Q* (MW)	Mean heat-recovery increments *dQ* (kW)	Mean percent heat-recovery increments *dQ* (%)	Mean outlet temperature increments dT_{CDend} (°C)	Average daily energy savings (MWh)	PID 1			PID 2		
						K_p	K_i	K_d	K_p	K_i	K_d
0	55.16	-	-	-	-	-			-		
1	55.02	-147.0	-0.27	-0.39	-	-			-		
2	55.75	+587.5	+1.07	+1.58	14.1	-1.9159	-0.0159	0	-3.3763	-0.0241	0
3	55.77	+605.3	+1.10	+1.63	14.5	-0.8175	-0.0082	0	-0.6042	-0.0068	0
4	55.61	+443.8	+0.81	+1.20	10.6	-0.1798	-0.0019	0	-0.4404	-0.0081	0

4. Conclusions

In this work, a real-life benchmark system comprising a HEN coupled with a CDU is considered. In such systems, the crude oil stream is typically split into parallel branches and the oil mass flows through the branches are kept in constant proportion (at constant split ratio) by the process control system. In this paper, simple linear control systems (PID controllers) were considered and among the studied control strategies, the best one was found to consist in adjusting the parallel flows so that identical temperature values are maintained at the outlets from two parallel branches and consequently, the heat recovery in the HEN is maximized. The simulations of closed-loop control were performed in MATLAB/Simulink environment and the results enabled comparative evaluation of the studied PID-control strategies and their potential to achieve energy savings in CDU operation. Compared to the strategy of constant split ratio, the strategy of equal outlet temperatures from the parallel network branches was found to increase the total heat recovery by about 1.1 %. During a selected period of CDU operation, the heat-recovery increment fluctuated in the range 100-1100 kW and the average daily energy saving was estimated at 14.5 MWh.

References

Bakošová M., Oravec J., 2014, Robust model predictive control for heat exchanger network, Applied Thermal Engineering, 73, 924–930.

Jäschke J., Skogestad S., 2014, Optimal operation of heat exchanger networks with stream split: only temperature measurements are required, Computers & Chemical Engineering, 70, 35–49.

Klemeš J.J., Varbanov P.S., 2013, Process intensification and integration: an assessment. Clean Technologies and Environmental Policy, 15(3), 417-422.

Markowski M., Urbaniec K., 2005, Optimal cleaning schedule for heat exchangers in a heat exchanger network, Applied Thermal Engineering, 25(7), 1019–1032.

Oravec J., Trafczynski M., Bakošová M., Markowski M., Mészáros A., Urbaniec K., 2017, Robust model predictive control of heat exchanger network in the presence of fouling, Chemical Engineering Transactions, 61, 337–342.

Skogestad S., 2003, Simple analytic rules for model reduction and PID controller tuning, J. Proc. Control, 13(4), 291–309.

Smith R., Loyola-Fuentes J., Jobson M., 2017, Fouling in heat exchanger networks, Chemical Engineering Transactions, 61, 1789–1794.

Trafczynski M., Markowski M., Alabrudzinski S., Urbaniec K., 2016, The influence of fouling on the dynamic behaviour of pid-controlled heat exchangers, Applied Thermal Engineering, 109, 727–738.

Varbanov P.S., Klemeš J.J., Friedler F., 2011, Cell-based dynamic heat exchanger models – Direct determination of the cell number and size, Comput. Chem. Eng., 35(5), 943–948.

Varga E.I., Hangos K.M., Szigeti F.,1995, Controllability and observability of heat exchanger networks in the time-varying parameter case, Control Eng. Pract., 3(10), 1409–1419.

Vasičkaninová A., Bakošová M., Mészáros A., Klemeš J.J., 2011, Neural network predictive control of a heat exchanger, Applied Thermal Engineering, 31, 2094–2100.